

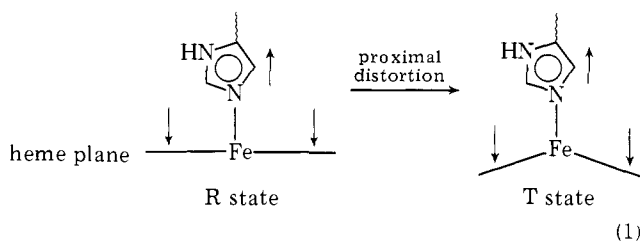
Model Compounds for R-State and T-State Hemoglobins<sup>1-3</sup>

Jon Geibel, John Cannon, Dwane Campbell, and T. G. Traylor\*

*Contribution from the Department of Chemistry, University of California, San Diego, La Jolla, California 92093. Received July 12, 1977*

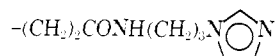
**Abstract:** Chelated heme compounds, in which an imidazole is covalently bound to a side chain of mesoheme so that the imidazole binds to iron without strain, have dioxygen and carbon monoxide binding kinetics and equilibria like those of R-state hemoglobin (HbX<sub>3</sub>). Strain is introduced into the Fe-imidazole bond by shortening the chelating ring or by attaching bulky groups to the imidazole or to the chelating ring. This strain increases the oxygen off rates and decreases oxygen affinity. These kinetic effects are similar to those observed in T-state hemoglobin (Hb) and are offered as evidence for the proposal that T-state hemoglobin derives at least part of its decreased oxygen affinity from proximal imidazole steric strain. The finding that this strain also brings about a change in the mechanism of carbon monoxide binding suggests that there are two possible T states of hemoproteins. One is a fast-reacting, low-affinity T state and the other is a slow-reacting, low-affinity T state.

Hemoglobin is usually regarded as a prototype of an allosteric protein.<sup>4,5</sup> Several general mechanisms have been proposed to explain the important phenomena of cooperativity in this molecular system.<sup>6-9</sup> All the proposals have in common the general idea that all four hemes are integral parts of the same conformational system. In the most detailed molecular mechanical model of the heme involvement in cooperativity, Perutz<sup>7</sup> has proposed that a movement of the proximal imidazole, perhaps with its attached iron, initiates the far-reaching conformational change in one of the subunits.<sup>7b</sup> This proposal is that some steric effect, either in the high-spin iron or in the protein itself, operates to pull the proximal imidazole away from the heme plane. When a ligand binds, this imidazole, with its appended protein helix, is pulled back into the plane of the heme. This tends to reverse whatever process pulled the imidazole away and sets off a series of conformational changes which find their way eventually to another heme to alter its reactivity by stabilizing its "in-plane" state. Presumably some steric pull or push, suggested by the arrows shown below, is operating to cause the deformation in the proximal imidazole direction.



It is therefore of interest to create, if possible, such deformation in model compounds and to study its effect upon the kinetics and equilibria of oxygen and carbon monoxide binding. The synthetic myoglobin active-site **1** (A, B = H; *n* = 3) (Figure 1), comprising a (five-coordinated) chelated heme, has the same electronic and geometrical properties as does hemoglobin,<sup>10a-d</sup> the same oxygen binding constant as does myoglobin<sup>5,11</sup> in water,<sup>10c</sup> and reacts by the same mechanism with carbon monoxide.<sup>2b,c</sup> We have therefore explored the possibility of introducing steric effects into our chelated heme **1**<sup>2c,10b</sup> to discover whether the same kinds of "proximal base pulling" effects as those proposed for hemoglobin would result in changing the synthetic site so that it behaves as does the T state of hemoglobin.<sup>12</sup>

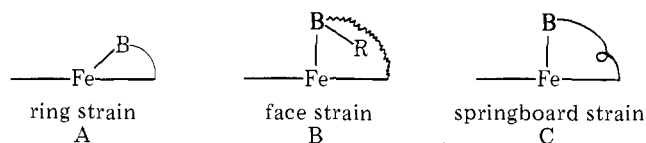
Because the ring structure involving:



was designed to be the smallest strain-free ring in this type of chelated heme,<sup>10b</sup> small changes in or on this side chain would

introduce strain in the ring and thus tend to pull the proximal imidazole away from the heme. This should introduce the kind of deformation suggested by Perutz.<sup>7</sup>

We have introduced strain in **1** in three ways, all designed to create forces which tend to move the "proximal" base away from the heme plane as illustrated below:



The reduction of *n* in Figure 1 from 3 to 2 causes the proximal base-iron-heme ring to be too small to achieve a strain-free conformation with consequent ring strain as illustrated in A. This effect introduces both Fe-N stretching and bending. The second kind of effect, face strain, is achieved without reducing the ring size but by merely introducing a bulky group, R, on the proximal base as shown in B. This approach has been used in the study of external base-heme mixtures, although effects are much smaller than those observed here.<sup>12b</sup> Still another way of introducing a force in the direction away from the heme plane is to introduce steric bulk in the heme-proximal base side-chain connection nearer to the heme edge. This effect, which we have called "springboard strain" in C, tends to spring open the heme-nitrogen connection without bending the Fe-N bond or introducing face strain. It is conceptually nearer to the kinds of pulling effect postulated to be introduced in the hemoglobin T state.

Referring to Figure 1, these changes have been made by reducing *n* to introduce ring strain, replacing H by CH<sub>3</sub> at A to introduce face strain, and replacing H by an alkyl group at B to cause the springboard strain effect. The different kinds of strain introduced by substitution of alkyl chains at positions A and B are clearly seen in a Corey-Pauling-Koltun (CPK) model of **1**. The hydrogen at position A is not only very close to the heme plane, but it is inside the chelate ring. Therefore, substitution of a methyl group for this hydrogen has an even larger repulsive effect in chelated hemes than in heme-external imidazole mixtures. Substitution of an alkyl group for the hydrogen at position B does not introduce direct repulsion with the heme plane, but demands conformational changes in the chelate ring which greatly strain the ring itself, resulting in a tendency to "spring open" the chelate ring. We have called this indirect destabilization of the iron-imidazole bond "springboard strain".

The alteration in kinetics and equilibria of ligand binding resulting from these strain effects reveals some surprising effects.

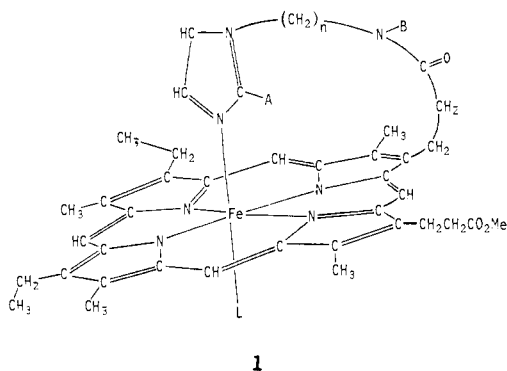


Figure 1. Chelated hemes having varying degrees of steric hindrance toward proximal base chelation. See Table I for individual structures.

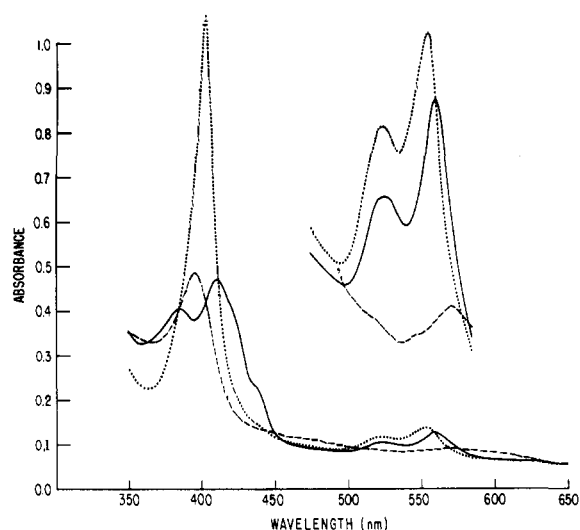


Figure 2. Spectra of 8  $\mu\text{M}$  mesohemin dimethyl ester derivatives in 2% aqueous cetyltrimethylammonium bromide (CetMe<sub>3</sub>NBr) containing 0.1 M potassium phosphate buffer at pH 7.3, 25 °C: oxidized ( $8^+ \text{Cl}^-$ ) (---); reduced with sodium dithionite (**8**) (—); after addition of 1 atm of CO (**8-CO**) (···). Insets are on  $A = 0-0.1$  scale.

## Results

**Syntheses.** The series of compounds listed in Table I was prepared from mono- or diacids of mesoporphyrin and purified by column chromatography to single-spot thin-layer chromatographic purity. Some of the previously studied compounds<sup>10a-d</sup> are included for reference.

**Kinetics of reactions with oxygen and carbon monoxide** were studied by flash photolysis as described by Gibson.<sup>11</sup> The rates of oxygen dissociation and association were derived from such flash photolysis kinetic determinations in mixtures of oxygen and carbon monoxide as previously described.<sup>10c</sup>

**Spectroscopy in Neutral Aqueous Suspension.** Because the first indication that the introduction of steric strain resulted in breaking the heme-proximal base bond came from spectroscopy,<sup>2b</sup> we will present the spectra of compounds **1-10** first.

Mesoheme dimethyl ester (**8**) has a spectrum in aqueous 2% cetyltrimethylammonium bromide (CetMe<sub>3</sub>NBr) buffer (Figure 2) which is identical with that in carefully dried benzene.<sup>12c</sup> Similarly, the chelated heme **1** has a spectrum in this medium (Figure 3)<sup>2c,3</sup> which is essentially identical with that of reconstituted mesoheme myoglobin. These spectra strongly suggest that neither four- nor five-coordinated hemes bind water when suspended in CetMe<sub>3</sub>NBr:

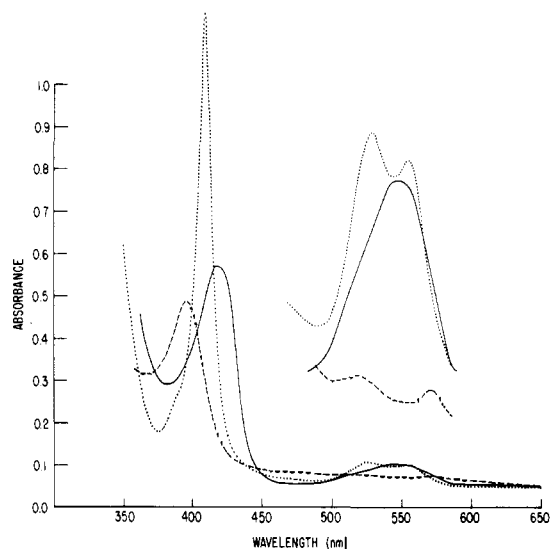
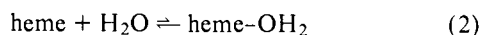


Figure 3. Spectra of 7  $\mu\text{M}$  mesohemin mono-3-(1-imidazolyl)propylamide monomethyl ester derivatives in the CetMe<sub>3</sub>NBr-buffer as described in Figure 2: oxidized ( $1^+ \text{Cl}^-$ ) (---); reduced (**1**) (—); carbon monoxide complex (**1-CO**) (···).

Table I. R- and T-State Hemoprotein Site Compounds Derived from Mesoporphyrin<sup>a</sup>

Compd	R <sub>1</sub>	R <sub>2</sub>
<b>1</b> <sup>2b,10d</sup>		OMe
<b>2</b> <sup>10d</sup>		
<b>3</b>		OMe
<b>4</b>		
<b>5</b>		OMe
<b>6</b>		OMe
<b>7</b>		OMe
<b>8</b>	OMe	OMe
<b>9</b>		OMe
<b>10</b>		OMe

<sup>a</sup> In this table and throughout the paper the structures are represented by numbers and the presence or absence of iron or its oxidation state is signified by following the number with P if the neutral porphyrin is indicated, with no symbol for the heme as it normally exists, with  $X^+$  for heme- $X^-$  derivatives, or with -CO, -O<sub>2</sub>, etc., for carboxy or oxy derivatives of heme, etc. For example, **1-CO** is the hexacoordinated CO derivative of **1** heme, **1-P** is the porphyrin, etc.

By contrast, compound **1** in methanol or water-methanol has a spectrum which is most clearly understood as a mixture of

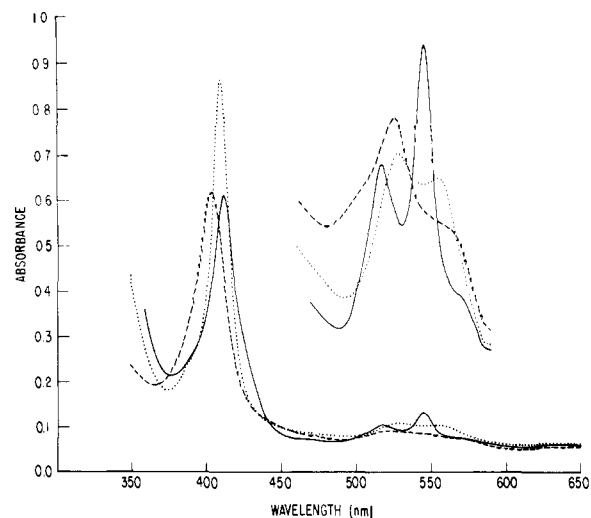
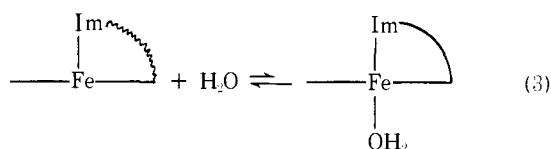


Figure 4. Spectra of 6  $\mu\text{M}$  mesohemin di-3-(1-imidazolyl)propylamide derivatives in the  $\text{CetMe}_3\text{NBr}$ -buffer solution taken as in Figure 2: oxidized ( $2^+\text{Cl}^-$ ) (- - -); reduced (**2**) (—); carbon monoxide complex (**2**-CO) (· · ·).

purely five-coordinated (myoglobin type) spectrum (see Figure 3) and hexacoordinated type spectrum (see Figure 4 for a typical hexacoordinated heme spectrum). In dimethylformamide and dimethyl sulfoxide the spectrum of **1** shifts further toward that of hexacoordinated heme at 25 °C. As the temperature is lowered to about -60 °C in these nucleophilic solvents the spectrum of **1** shifts to that of complete hexacoordination.<sup>10a,13</sup> These results demonstrate that, although alcohols, water, etc., combine weakly to five-coordinated chelated hemes, water shows little tendency to do so in  $\text{CetMe}_3\text{NBr}$  suspension:



This suggests that  $\text{CetMe}_3\text{NBr}$  suspension satisfies this aspect of the hemoprotein active site. The large differences in the spectra of the four-, five-, and six-coordinated hemes in Figures 2, 3, and 4 show that appreciable dissociation of the five-coordinated heme to four-coordinated would be detected as a spectral change in both the Soret and the visible regions in this solvent.

The spectra of deoxy, oxidized, and carbonmonoxy **1**, **5**, and **6** in the Soret region are shown in Figure 5. These three spectra are almost identical and even the strained compounds **5** and **7** (Figure 6) show no indication of appreciable four-coordinated heme in  $\text{CetMe}_3\text{NBr}$ -buffer at pH 7.3.

Contrasting results were obtained with compounds **3** and **4**. The spectra of **3** and **4** are shown in Figures 7 and 8. The appearance of the  $\alpha$  band at 556 nm in **3** is typical of four-coordinated heme shown in Figure 2 and indicates 20–30% four-coordinated heme in the  $\text{CetMe}_3\text{NBr}$ -aqueous buffer system. The spectrum of **4** in this same region indicates much less four-coordinated heme, to be expected as a result of having twice the local concentration of imidazoles. There is also no sign of hexacoordinated heme in the spectrum of **4**, in agreement with the results of Brault and Rougee,<sup>12d</sup> who found no hexacoordinated heme upon treatment of deuteroheme with 2-methylimidazole.

However, unlike external 1,2-dimethylimidazole or 2-methylimidazole which bind to heme better ( $K_3$  larger) than does 1-methylimidazole in water,<sup>2c,14</sup> the internally bound

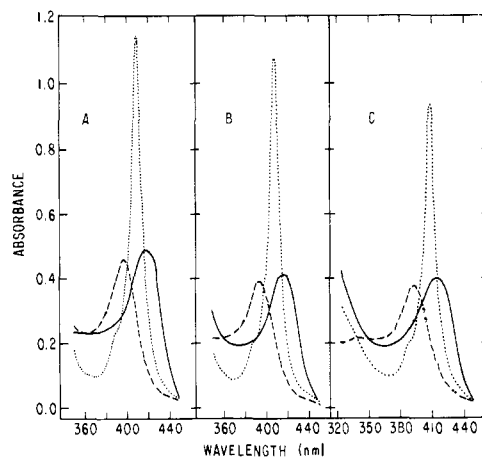


Figure 5. Soret region spectra of chelated hemes ( $\sim 6 \mu\text{M}$ ) shown in Figure 1, having  $n = 2, 3$ , and 4, and A, B = H (note **5** utilizes ester linkage) under the same conditions as those in Figure 2: oxidized (- - -); reduced (—); carbon monoxide complex (· · ·); (A) mesohemin mono-2-(1-imidazolyl)ethyl ester monomethyl ester ( $5^+\text{Cl}^-$ , **5**, **5**-CO); (B) mesohemin mono-3-(1-imidazolyl)propylamide monomethyl ester ( $1^+\text{Cl}^-$ , **1**, **1**-CO); (C) mesohemin mono-4-(1-imidazolyl)butylamide monomethyl ester ( $6^+\text{Cl}^-$ , **6**, **6**-CO).

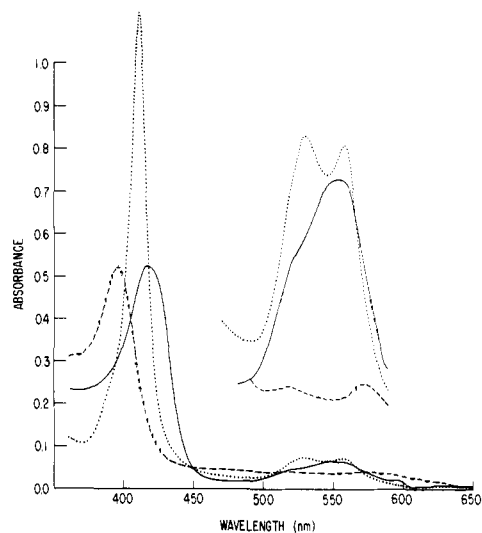
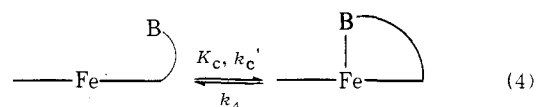


Figure 6. Spectra of mesohemin mono[bis[3-(1-imidazolyl)propyl]amide] monomethyl ester derivatives in  $\text{CetMe}_3\text{NBr}$ -buffer as in Figure 2: oxidized ( $7^+\text{Cl}^-$ ) (- · -); reduced (**7**) (—); carbon monoxide complex (**7**-CO) (· · ·).

2-methylimidazole compounds apparently bind poorly ( $K_c$  smaller) compared to the unhindered imidazole in **1**. This effect is seen very clearly in the compound **10** which shows only four-coordination in  $\text{CetMe}_3\text{NBr}$  suspension even though external 2-methylpyridine binds to hemes.<sup>13,14</sup>



The spectra of **7**,  $7^+\text{Cl}^-$ , and **7**-CO (Figure 6) in  $\text{CetMe}_3\text{NBr}$ -buffer at pH 7.3 are almost identical with the corresponding spectra of **1**,  $1^+\text{Cl}^-$ , and **1**-CO (Figure 3) revealing no more spectrally detectable four-coordinated heme form present in a solution of **7** than in similar solutions of **1**.

**pH Dependence of Spectra.** One of the measurements of the equilibrium between iron-bound and free imidazole in such covalently bound models as **1**, **3**, etc., is the pH-affected change from five-coordination to four-coordination (eq 5 and 6) as

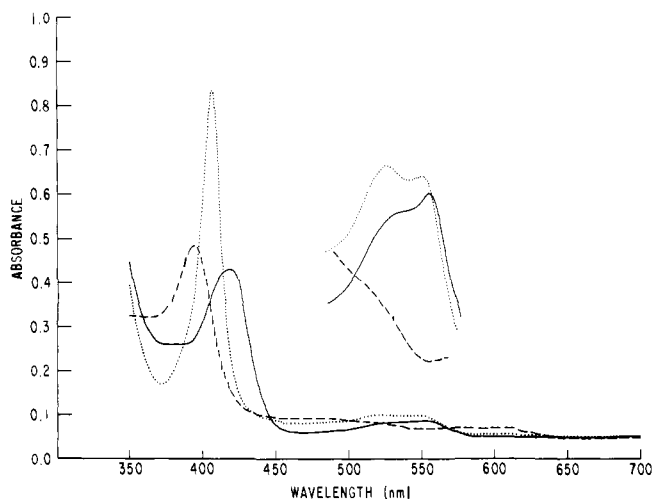


Figure 7. Spectra of mesohemin mono-3-[1-(2-methyl)imidazolyl]propylamide monomethyl ester derivatives in  $\text{CetMe}_3\text{NBr}$ -buffer as described in Figure 2: oxidized ( $3^+\text{Cl}^-$ ) (---); reduced (**3**) (—); carbon monoxide complex (**3-CO**) (···).

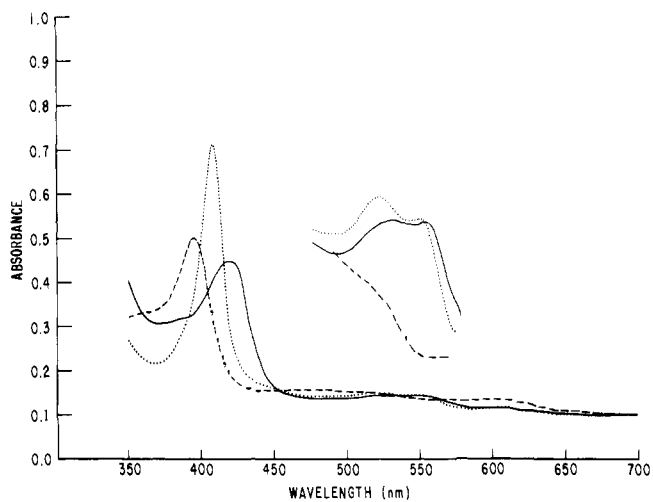
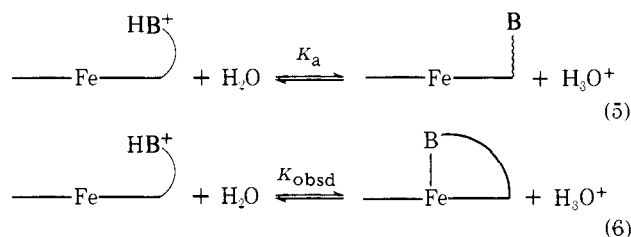


Figure 8. Spectra of mesohemin di-3-[1-(2-methyl)imidazolyl]propylamide derivatives in  $\text{CetMe}_3\text{NBr}$ -buffer as described in Figure 2: oxidized ( $4^+\text{Cl}^-$ ) (---); reduced (**4**) (—); carbon monoxide complex (**4-CO**) (···).



indicated by the change in spectra judged from the distinct spectra in Figures 2 and 3.

The spectra of **1** in  $\text{CetMe}_3\text{NBr}$ -buffer at pH values from 9 to 3.5 are shown in Figure 9. Although some oxidation obscures the spectrum at pH 3.6, there is clearly appreciable five coordinated heme remaining at pH 3.6 and essentially complete five-coordination at pH 5.5. These data indicate half-conversion at about pH 3.6.

By contrast, the spectra of the hindered compound **3** show essentially complete conversion from five- to four-coordination at pH 5.8 and half-conversion at pH 6.6 (Figure 10). The  $pK_a$  of 1-(3-acetamidopropyl)-2-methylimidazole, a close chemical analogue of the uncomplexed form of **3**, was measured to be 7.6 in water. This small change from  $pK_a = 7.6$  to  $pK_{\text{obsd}} = 6.6$

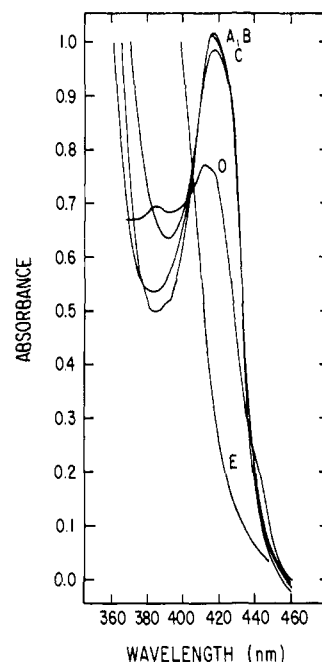


Figure 9. Soret region spectra of **1** in 2%  $\text{CetMe}_3\text{NBr}$ -buffer containing approximately 0.1 M phosphate buffers at various pH values. pH values were: (A) 9; (B) 5.5; (C) 4.5; (D) 3.5; (E) 2.0.

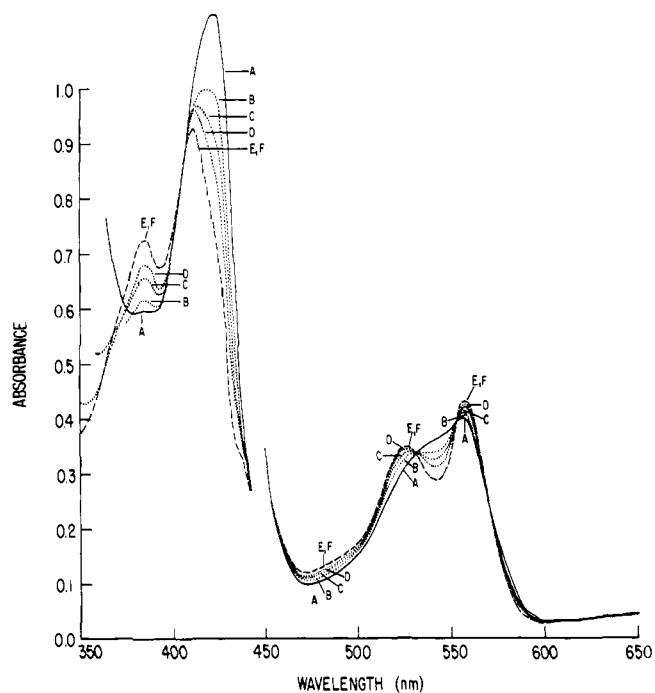


Figure 10. Spectra of mesoheme mono-3-[1-(2-methyl)imidazolyl]propylamide monomethyl ester (**3**) in  $\text{CetMe}_3\text{NBr}$ -buffer at various pH values. pH values were: (A) 8.5; (B) 6.7; (C) 6.3; (D) 6.0; (E) 5.3; (F) 4.3.

reveals, after correction for the amount of four-coordinated heme present at high pH, a  $K_c \approx 10$  compared to a  $K_c \approx 800$  for **1**, determined by a similar comparison.<sup>2b</sup> However, see the discussion below for correction of these figures for the effects of  $\text{CetMe}_3\text{NBr}$ .

Similar effects of hindrance in **3** are seen in the carbon monoxide complex **3-CO**. While the spectrum of **1-CO** remains unchanged from pH 9 to 2, the spectrum of **3-CO** changes from that of hexacoordination at pH 9.9 to that of five-coordinated (base off) CO complex at 3.7 with a half-point at pH  $\approx 6$  (see

**Table II.** Rate Constants for Reaction of CO or O<sub>2</sub> with Chelated Heme Compounds in CetMe<sub>3</sub>NBr-Buffer at 23 °C<sup>a,b</sup>

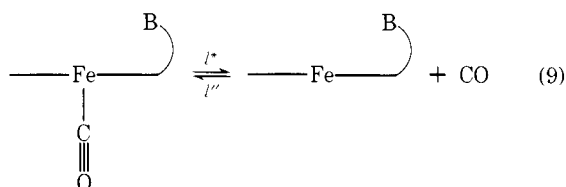
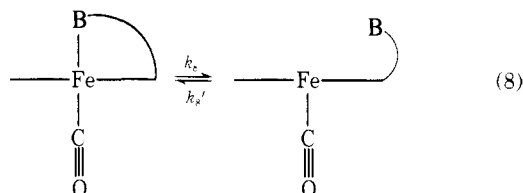
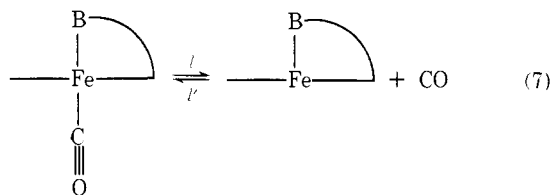
Heme compd	$l'$ , $M^{-1} s^{-1}$ $\times 10^{-7}$	$k'$ , $M^{-1} s^{-1}$ $\times 10^{-7}$	$k$ , $s^{-1}$	$K_{O_2}$ , $k'/k$ , $M^{-1} \times 10^{-6}$
1	1.1 <sup>c</sup>	2.2	23	1.0
2	0.22	<i>d</i>		
3	12	<i>e</i>		
4	8	<i>e</i>		
5	2.3	4.9	160	0.3
6	1.5	2.9	24	1.2
7	4.8	4.7	140	0.34
8	30	<i>e</i>		

<sup>a</sup> All rates were determined by flash spectroscopy in 0.1 F phosphate buffer at pH 7.3 containing 2.0% cetyltrimethylammonium bromide and are reproducible between experiments to  $\pm 10\%$ . <sup>b</sup>  $l'$  and  $k'$  are the bimolecular rate constants for reaction with CO and O<sub>2</sub>, respectively, and  $l$  and  $k$  are the dissociation rate constants. <sup>c</sup> This value was determined at pH 9. The  $l'$  for **1** is  $1.2 \times 10^7 M^{-1} s^{-1}$  at pH 7.3. <sup>d</sup> The second imidazole in this compound as in external imidazole heme compounds interferes with the CO/O<sub>2</sub> competition method of determining  $k$ . <sup>e</sup> This compound was very quickly oxidized even in the presence of carbon monoxide.

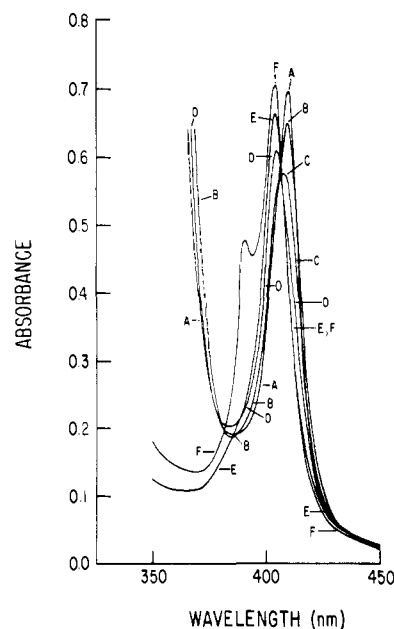
Figure 11). This closure constant can thus be calculated to be only four times that of **3** itself.

**Kinetics and Equilibria.** Having shown that **1** binds carbon monoxide by different mechanisms at  $pH \geq 7$  or  $pH \leq 3.2^c$  and that four-coordinated heme **8** binds carbon monoxide about 30 times faster than does five-coordinated heme **1** in water,<sup>2b</sup> we can now use the kinetics of CO binding in **2–7** to indicate mechanisms of reaction. The rates of reaction of carbon monoxide or oxygen with the variously hindered hemoprotein site models are listed in Table II. This table also indicates an instability of the oxyheme toward dissociation resulting from proximal base strain. This instability results from an increased dissociation rate.

The faster rates of reaction of carbon monoxide with **3**, **4**, and **7** than with **1** correspond to a change in mechanism from direct association (eq 7) to base elimination (eq 8, 9, and 4).



The strain in compounds **3** and **4** apparently causes breaking of the iron-imidazole bond. In particular, the rate constant for the reaction of carbon monoxide with **3** in CetMe<sub>3</sub>NBr-buffer at pH 8.5 is about one-fourth that of the reaction of pure four-coordinated heme, **8**, under the same conditions. This agrees with the determination of the ratio of five-coordinated



**Figure 11.** Spectra of mesoheme mono-3-[1-(2-methyl)imidazolyl]propylamide monomethyl ester carbon monoxide complex (**3**-CO) under 1 atm of carbon monoxide in the CetMe<sub>3</sub>NBr-buffer of Figure 2 at various pH values. pH values were: (A) 9.9; (B) 7.6; (C) 6.4; (D) 5.6; (E) 3.7; (F) 3.6.

to four-coordinated heme in **3** of about 10 estimated from the pH-spectral correlations discussed above.

**pH-Rate Profiles.** Another measure of the equilibrium constant for proximal base binding to iron is the pH-rate profile for carbon monoxide, reported previously.<sup>2b</sup> Assuming the dual mechanism scheme **7–9**, the observed rate constant for the carbon monoxide reaction ( $l'_{\text{obsd}}$ ) with a monobase compound such as **1**, **3**, **5**, or **6** can be expressed as a function of the rate constant for five-coordinated heme ( $l'$ ) (eq 7), the rate constant for four-coordinated heme ( $l''$ ) (eq 9), the chelation constant ( $K_c$ ) (eq 4), and the acidity of the uncomplexed, protonated imidazole ( $K_a$ ) (eq 5):




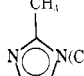
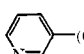

$$\log \left( \frac{l'' - l'_{\text{obsd}}}{l'_{\text{obsd}} - l'} \right) = \text{pH} - \text{p}(K_a K_c) \quad (10)$$

The side-chain bases (R<sub>1</sub>-H) in **1**, **3**, **5**, and **6** were acetylated and  $\text{p}K_a$  values of these substituted imidazoles were used as  $\text{p}K_a$  values for the uncomplexed bases in the hemes according to eq 5. A plot of eq 10 for **1** is shown in Figure 12, and the bases, their  $\text{p}K_a$  values, and derived values of  $\text{p}K_c$  are shown in Table III.

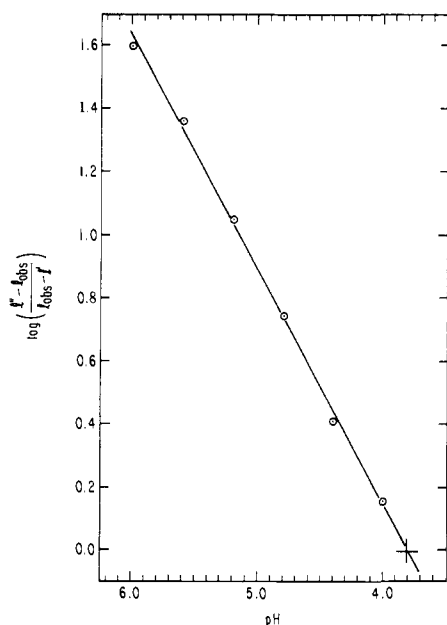
The evaluation of the closure constants  $K_c$  for compounds in Table III rests upon several assumptions. First, it is assumed that the open, unchelated form of the heme has the same  $\text{p}K_a$  of its appended imidazole as does its model base shown in Table III.<sup>2b,c</sup> Secondly, it is assumed that all open protonated or unprotonated forms of mesoheme derivatives react with carbon monoxide with the same rate constant as does **8**. It is also assumed, with some justification,<sup>15</sup> that proton transfer to imidazoles in acid ( $\text{pH} < 4$ ) is fast compared to the reaction of carbon monoxide, and that the  $\text{p}(K_c K_a)$  derived from eq 10 corresponds to the protonation of the proximal base (eq 4 and 5).

Because the  $\text{p}K_a$  of the model imidazoles was measured in water and our  $\text{p}K'$  in CetMe<sub>3</sub>NBr-buffer, we must make some correction for the effect of CetMe<sub>3</sub>NBr on  $\text{p}K_a$  values of monopositively charged acids. This effect can be as large as 1  $\text{p}K$  unit.<sup>16</sup> We estimate the effect by comparing the  $K_c$  for compound **3** determined by examining the spectrum at pH 9 (in comparison with the four- and five-coordinated heme spectra)

**Table III.** Observed  $pK'$  for Protonation of Base-Heme Model Compounds as Determined from pH-Rate Profiles

Model base	$pK_a$	Heme	$pK'$	$-pK_c$	$K_c$	Ref
 (11)	6.57 (6.07) <sup>a</sup>	<b>1</b>	3.64	2.93	850 (250) <sup>a</sup>	2b This work
 (12)	6.11 (5.6) <sup>a</sup>	<b>5</b>	3.52	2.59	390 (120) <sup>a</sup>	This work
 (13)	6.59 (6.1) <sup>a</sup>	<b>6</b>	3.71	2.88	760 (230) <sup>a</sup>	This work
 (14)	7.6 (7.1) <sup>a</sup>	<b>3</b>	~6.6		10 (3) <sup>b</sup>	This work
 (15)	5.11 (4.6) <sup>a</sup>	<b>9</b>	1.40	3.71	5100 (1500) <sup>c</sup>	2b This work
 (11)	6.57 (6.07) <sup>a</sup>	<b>7</b>			~10 <sup>b</sup>	

<sup>a</sup> The  $pK_a$  values and resulting  $K_c$  values in parentheses are corrected for the  $\Delta pK_a \cong 0.5$  effect of  $\text{CetMe}_3\text{NBr}$  on acid dissociation (see text). <sup>b</sup> Calculated by assuming that the observed rate constant for **7** is a sum of the rate constants observed for **1** and **8** times the respective mole fractions,  $l'_{\text{obsd}} = l_8''F_o + l_1'F_c$  where  $F_o$  and  $F_c$  are mole fractions for the open and closed forms of **7**.



**Figure 12.** Plot of pH-rate profile for the rates of carbon monoxide reaction with **1** in  $\text{CetMe}_3\text{NBr}$ -buffer according to eq 10. The values of  $l'' = 3.0 \times 10^8 \text{ M}^{-1} \text{ s}^{-1}$  and  $l' = 1.1 \times 10^8 \text{ M}^{-1} \text{ s}^{-1}$  were previously determined.<sup>10d</sup>

(or by comparing  $l'_{\text{obsd}}$  for **3** with that of **8** at the same pH), with the  $K_c$  determined by pH titration. A comparison of the visible spectrum of **3** at pH 7.3 (Figure 7) with that of the five-coordinated complex of 2-methylimidazole (0.2 M) and **8** in the same solution and with the spectrum of **8** (Figure 2) indicates that about 30% of **3** exists in the four-coordinated form in  $\text{CetMe}_3\text{NBr}$ -buffer. The rate of carbon monoxide reaction with **3**,  $l' = 1.2 \times 10^8 \text{ M}^{-1} \text{ s}^{-1}$ , compared to the rate with the four-coordinated heme **8**,  $l'' = 3 \times 10^8 \text{ M}^{-1} \text{ s}^{-1}$  at pH 7.3, reveals a  $K_c \cong 3$ . Taking this value of  $K_c$  we calculate an error factor of  $10/3 = 3.3$  ( $\Delta pK_a = 0.5$ ) in the pH-titration or pH-rate profile methods employed in  $\text{CetMe}_3\text{NBr}$ -buffer. This correction arises from our having measured  $pK_a$  values in water rather than in  $\text{CetMe}_3\text{NBr}$ . Corrected values of  $K_c$  are shown in parentheses in Table III. These corrections lower the values of  $K_c$  but do not affect the conclusions of this study. Values in parentheses are lower limits of  $K_c$ .

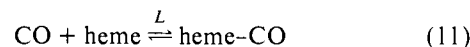
**Table IV.** Carbon Monoxide Titration of Heme Compounds in Aqueous  $\text{CetMe}_3\text{NBr}$ -Buffer

Heme	$L$ , $\text{M}^{-1} \times 10^{-6}$
<b>1</b>	600 <sup>a,b</sup>
<b>3</b>	3.1
<b>8</b>	0.6 <sup>c</sup>

<sup>a</sup> From ref 10f as determined by kinetic methods. Titration<sup>14</sup> indicates  $L \gg 10^8 \text{ M}^{-1}$ . <sup>b</sup> We previously reported a much lower value of  $L^{10e}$  which we have found to be incorrect.<sup>10b</sup> <sup>c</sup> Reference 14.

We have previously shown that  $k_4'$  and  $k_4$  are very fast ( $\gg 10^3 \text{ s}^{-1}$ ).<sup>2c,3</sup> We also have strong evidence that **1** reacts with CO predominantly by the association mechanism at  $\text{pH} \geq 7$  and by base elimination at  $\text{pH} \leq 4$ .<sup>2b,c</sup> We can therefore conclude that  $l' = 1.1 \times 10^7 \text{ M}^{-1} \text{ s}^{-1}$  can be taken as the rate of reaction of unstrained five-coordinated heme with carbon monoxide and that  $3 \times 10^8 \text{ M}^{-1} \text{ s}^{-1}$  is a good estimate for the reaction rate constant with four-coordinated heme.

The effect of introducing the extreme steric hindrance in **3** upon the carbon monoxide equilibrium constant was determined by titrating **3** and **8** with carbon monoxide in  $\text{CetMe}_3\text{NBr}$ -buffer at pH 7.3:



The resulting  $L$  values are listed in Table IV. Thus, this R  $\rightarrow$  T change in the **1**  $\rightarrow$  **3** heme change, while increasing  $l'_{\text{CO}}$ , greatly decreases the  $L_{\text{CO}}$ .

## Discussion

The original synthetic myoglobin site **1a**,<sup>10b</sup> having a three-carbon amide chelating chain, reacts with carbon monoxide and with oxygen with rate constants which are almost identical with those of the longer side-chain compound **6** (Table II). Therefore, we can safely assume that the site **1** has no iron-base strain in excess of that which is inherent in an imidazole-heme bond due to imidazole-hydrogen-porphyrin repulsion<sup>17</sup> or iron radius repulsion,<sup>18</sup> both of which tend to cause the iron to move out of the heme plane. In particular, the identical oxygen off rates  $k$  for **1** and **6** suggest that, as hexacoordinated species, these compounds are also similarly strained (or unstrained). These two compounds can therefore be taken as R-state models of a hemoglobin site.<sup>10d</sup>

**Table V.** Fraction of Four-Coordinated Heme and Fraction of Reaction Proceeding through Four-Coordinated Heme in Strained Site Models<sup>a</sup>

Heme	$F_{\text{open}}$	$(1 - F_A)$
<b>1</b>	[0] (0.004) <sup>b</sup>	[0] (0.1) <sup>b</sup>
<b>3</b>	0.4	0.95
<b>4</b>	0.2	0.9
<b>7</b>	0.1	0.8

<sup>a</sup> In  $\text{CetMe}_3\text{NBr}$ -0.1 M phosphate buffer at 23 °C. <sup>b</sup> Calculated from  $K_c$  in Table III. All other values were calculated from eq 12.

Upon introducing proximal strain (e.g., springboard strain) into chelated hemes, both dioxygen and carbon monoxide binding constants are reduced. This confirms the postulate that out-of-plane forces upon the heme iron reduce binding affinity.<sup>7</sup> Therefore, the strained compounds **3**, **5**, and **7** are models for the hemoglobin T state. Substitution of one of the imidazoles in **7** with a phenyl group, which maintains the steric effect but halves the local imidazole concentration, produces a compound having the same oxygen off rate as does **7**.<sup>10h</sup> We can therefore conclude that this dissociation takes place without prior dissociation of the imidazole, i.e., by the direct association-dissociation mechanism.<sup>10d</sup> This makes the oxygen binding mechanism for these T-state models very like those usually proposed for hemoproteins.

By contrast, introduction of strain into these T-state models **3**, **5**, and **7** not only decreases carbon monoxide binding but changes its mechanism of binding from that of direct association (eq 7) to one of base elimination (eq 8 and 9). Using the rate constants for CO reaction with mesoheme dimethyl ester (**8**) and the R-state site **1** as four- and five-coordinated heme rate constants, respectively,  $l_4'' = 3 \times 10^8 \text{ M}^{-1} \text{ s}^{-1}$  and  $l_5' = 1.1 \times 10^7 \text{ M}^{-1} \text{ s}^{-1}$ , we can calculate the fraction of four-coordinated heme ( $F_{\text{open}}$ ) and the fraction of reaction ( $F_A$ ) proceeding through the association mechanism and that proceeding through the base elimination mechanism ( $1 - F_A$ ) for each of the strained compounds, assuming that  $l_5'$  for the closed compound is identical with that of **1**. Because  $l_5'$  would likely be less than  $1.1 \times 10^7 \text{ M}^{-1} \text{ s}^{-1}$ ,<sup>14</sup> this method calculates a minimum possible value of  $F_{\text{open}}$ :

$$F_{\text{open}} = \frac{k - l_5'}{l_4'' - l_5'} = \frac{10^{-7}k - 1.1}{29} \quad (12)$$

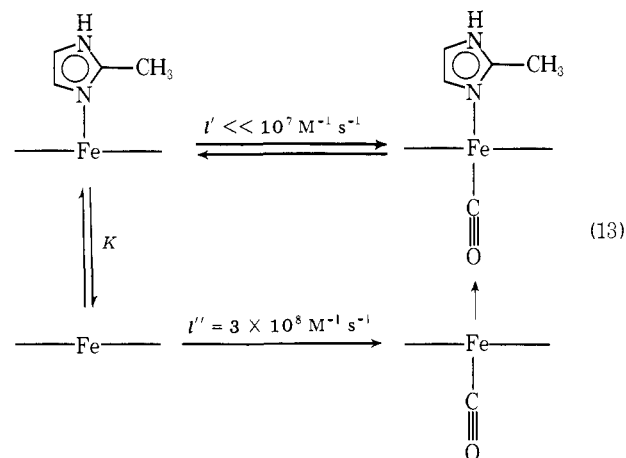
The fraction  $F_{\text{open}}$  calculated from eq 12 is listed in Table V along with  $F_A$ , the fraction of the deoxy heme existing as four-coordinated heme in this solvent.

It is clear from Table V that at least two of the three kinds of strain have shifted the heme-base equilibria to such an extent that the reaction with CO proceeds predominantly by the base-elimination mechanism. We have therefore established one effect of the proposed T-state pull on the proximal base. The proximal base iron bond is simply broken and the mechanism changed. Why is this not seen in the spectra? As Table V shows, only 10% four-coordinated heme is required to bring about 80% base-elimination mechanism and an increase of more than a factor of three in rate. This is because four-coordinated heme reacts faster than five-coordinated heme.

The mechanism change upon changing structure **1** to **7** demonstrated in Table V in  $\text{CetMe}_3\text{NBr}$ -buffer has also been observed to occur in 50% methanol- $\text{H}_2\text{O}$ ,<sup>14</sup> so that the results reported here are not peculiar to the  $\text{CetMe}_3\text{NBr}$  suspension. Kinetic behavior in  $\text{CetMe}_3\text{NBr}$ -buffer resembles that in aqueous-organic solvent mixtures.<sup>10c</sup>

A change from the association mechanism to base elimination generally results in increases in both on and off rates of CO binding<sup>2c</sup> with the larger change in the off rate and consequent decrease in binding constant (compare  $l'$  and  $L$  for

**3**). Thus, a proximal base pull can result in increased on and off rates due to a mechanism change. But an entirely different mechanistic effect of, e.g., face strain is possible. We have reported,<sup>2c</sup> and will discuss further in a subsequent paper, the kinetics of carbon monoxide reaction with heme-2-methylimidazole mixtures. This study shows that at high (>1 M) concentrations of 2-methylimidazole or 1,2-dimethylimidazole very little hexacoordinated heme is present,<sup>12b</sup> but the fraction of pentacoordinated heme is very high and that of four-coordinated heme is very low. The result that the observed rate constant for reaction of this mixture with carbon monoxide is much less than that of **1** indicates that five-coordinated heme, having a hindered imidazole, reacts much more slowly with CO by the association mechanism than does strain-free (R state) five-coordinated heme.<sup>2c</sup>



Although the equilibrium constant indicated in eq 13 is independent of the mechanism employed, the kinetics are not, and kinetic behavior reveals much about the process and the way in which equilibria are altered.

It seems clear that a reduction in the equilibrium constant for carbon monoxide binding to hemoproteins could be achieved by proximal base strain through either the direct-association or base-elimination mechanism. The observation that the entire heme moves within the pocket upon binding CO to hemoglobin A<sup>19</sup> or chironimus hemoglobin<sup>20</sup> suggests that the heme movement, required by the proximal base elimination mechanism, is possible in hemoproteins. The recent observation<sup>21,22</sup> that nitrosyl hemoglobin A displays breaking of the iron-proximal imidazole bond also suggests that CO binding could proceed through such base elimination in hemoproteins. We have recently found<sup>23</sup> that myoglobin has a pH-rate profile for reaction with CO which is very similar to that reported for **1**, indicating that myoglobin reacts by base elimination below  $\text{pH} \approx 3$  just as does the chelated heme **1**.

While we have shown that the effects of proximal base steric changes can be large and could account for some of the kinetic differences between R- and T-state hemoglobins, we cannot ignore the distal side steric effects in hemoprotein pockets, which our models do not possess. For example, in contrast to the usual linear metal carbonyl bonds,  $\text{M-CO}$ ,<sup>18b</sup> the C-O group in carboxy derivatives of hemoglobin A,<sup>19</sup> chironimus hemoglobin,<sup>20</sup> and myoglobin<sup>24</sup> are inclined about 30° from the preferred perpendicular direction, presumably due to some steric hindrance.<sup>19,25</sup> Although it is expected that such bending would be reflected in the ligand binding, there appears to be no correlation between this bending, at present accuracy, and the kinetics or equilibria of CO binding. Myoglobin<sup>24</sup> and chironimus hemoglobin<sup>20</sup> show similar Hm-CO distortion, but chironimus hemoglobin binds CO with about 10 times higher equilibrium constant and much faster than does myoglobin.<sup>26</sup> But oxygen, whose binding is presumably less sensitive to distal side steric effects,<sup>25</sup> is bound to these two proteins with ap-

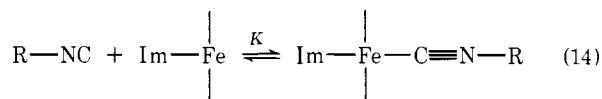
Table VI. Proposed Effects of Proximal Strain and Distal Steric Hindrance on the Kinetics of Heme Reactions with CO and O<sub>2</sub>

Heme	Proximal strain	Distal hindrance	$l'$ , M <sup>-1</sup> heme s <sup>-1</sup>	$l$ , s <sup>-1</sup>	$k'$ , M <sup>-1</sup> heme s <sup>-1</sup>	$k$ , s <sup>-1</sup>	Ref
<b>1</b>	None	None	$1.1 \times 10^7$	0.015 <sup>a</sup>	$2 \times 10^7$	23	This work
$\alpha$ chain	None	Little	$4 \times 10^6$	0.016	$5 \times 10^7$	30	28, 29
Legoglobin	None	Little	$1.3 \times 10^7$	0.012	10 <sup>8</sup>	10 (4)	30, 31
Myoglobin	None	Large	$5 \times 10^5$	0.017	$1.5 \times 10^7$	10	5
HbX <sub>3</sub>	None	Little	$6 \times 10^6$	0.03	$4 \times 10^7$	12.5 <sup>b</sup>	33, 34
Hb	Large	Little	10 <sup>5</sup>	0.09	10 <sup>7</sup>	1050	33, 34
<b>7<sup>c</sup></b>	Medium	None	$4.8 \times 10^7$		$4.7 \times 10^7$	140	This work
<b>3<sup>c</sup></b>	Large	None	$1.2 \times 10^8$				This work
Chironimus Hb <sup>c</sup>	Medium	None	$3 \times 10^7$	0.09	$3 \times 10^8$	218	26

<sup>a</sup> Reference 10f. <sup>b</sup>  $k_4$  per heme. <sup>c</sup> These hemes are thought to react with CO by base-elimination mechanisms.

proximately equal binding constants. We conclude that the CO complex geometry is not a very good indication of the "openness" of the heme pocket.

Another probe of pocket size, which might better relate to ligand binding dynamics, is the binding kinetics and equilibria of isonitriles of varying size.



Chironimus hemoglobin and isolated hemoglobin A chains bind isonitriles more strongly than does myoglobin.<sup>26,27</sup> This difference between chironimus hemoglobin and myoglobin increases as R size in RNC increases from Me to Et, *i*-Pr, *t*-Bu.<sup>27</sup> As judged by ligand binding, chironimus hemoglobin and isolated hemoglobin A chains have more "open" pockets than does myoglobin.

This conclusion is strengthened by the observation that the rates of carbon monoxide reaction with hemoglobin  $\alpha$  chains,<sup>28,29</sup> legoglobin,<sup>30,31</sup> and chironimus hemoglobin are comparable to that of chelated heme **1** in CetMe<sub>3</sub>NBr-buffer. We can therefore equate the kinetic behavior of our unstrained chelated heme in CetMe<sub>3</sub>NBr suspension to that of unstrained (R-state type) hemoproteins having open and thus unstrained distal side pockets.

The first step in CO binding to hemoglobin A has a slow ( $10^5 \text{ M}^{-1} \text{ s}^{-1}$ )<sup>32</sup> on rate constant and a fast ( $0.09 \text{ s}^{-1}$ )<sup>33</sup> off rate constant compared to the last step in which the on and off rates approach those of the standard, presumably open, relaxed compounds (Hb  $\alpha$  chains,<sup>28,29</sup> legoglobin,<sup>30,31</sup> compound **1**). These kinetic results could be obtained from the R- and T-state model kinetics in two distinctly different but not exclusive ways.

(1) Hemoglobin could somehow respond to ligation by opening up the cavity on the distal side of the subsequently binding hemes. This would convert the myoglobin-like structure, in which CO reacts slowly, to the open, unhindered pocket leading to larger on rates like those in legoglobin or chironimus hemoglobin. The problem with the distal side explanation is that it offers no logical reason for rapid dissociation from Hb<sub>4</sub>CO.<sup>33</sup>

(2) Hemoglobin could remain in the open pocket conformation during all four ligation steps and alter the kinetics in each step by introducing varying amounts of face strain or pull strain. Such strain could easily cause the CO off rate  $l_1$  to increase whether the proximal base bond breaks first or not ( $l$  increases with increasing face strain in synthetic hemoprotein sites).<sup>10f</sup>

If this strain broke the proximal base-heme bond the  $l_1'$  would be faster than  $l'$  for R-state models such as **1**. This is not observed. It therefore seems that the simplest rationale is that, in the T state, hemoglobin somehow achieves the "high local imidazole concentration" discussed above and maintains the

association mechanism even in the presence of considerable pulling strain; that is, T-state hemoglobin A reacts with CO by predominant direct-association mechanism.

A combination of methods 1 and 2 cannot be excluded but invoking distal side steric effects to explain cooperativity is not justified by our present results.

These postulates lead to some rather odd conclusions. For example, we are led to conclude that myoglobin,  $\alpha$  chains, and legoglobin are all rather similar R-state hemoproteins like R-state hemoglobin and **1** (in CetMe<sub>3</sub>NBr suspension) even though their rates of reaction with CO vary greatly. This on-rate variation is best explained in terms of distal side steric hindrance causing the on rate to be retarded without greatly changing the off rate. Therefore, myoglobin, though in the R state, reacts slowly because CO is either encountering steric hindrance to pocket entry or to proper orientation for binding. This apparently means that T-state hemoglobin and myoglobin react slowly with CO for different reasons. Some of the pertinent rate constants and the possible sources of their differences from those of the standard R-state synthetic site **1** are shown in Table VI.

One of the interesting things which is apparent from Table VI, and has been noticed before, is that neither the proximal strain nor the hindrance affects the O<sub>2</sub> on rate ( $k'$ ) very much. This is consistent with the "charge-transfer" type of early transition state<sup>10c,33</sup> for O<sub>2</sub> binding in which perhaps an O<sub>2</sub><sup>-</sup>·Fe<sup>+</sup> pair forms at some distance, reducing the steric effects upon the O<sub>2</sub> on rates.

But the oxygen off rates do appear to be affected by strain, both the strained **5** and **7** showing enhanced off rates, even though CO kinetics are unaffected by the strain in **5**. This suggests that the fast O<sub>2</sub> off rates for T-state hemoglobin and for chironimus hemoglobin result from proximal strain, but the kinetics of CO binding to chironimus hemoglobin are more compatible with a base-elimination mechanism for CO reactions similar to that which has been demonstrated for **3** and **7**.<sup>2c</sup> We think that, with regard to carbon monoxide, perhaps there are both fast reacting and slow reacting "T-state" hemoprotein sites.

## Conclusion

Introduction of proximal base strain into hemoprotein model compounds decreases their affinity for both dioxygen and carbon monoxide. This confirms the proposal that such strain could contribute to the differences in affinity of R- and T-state hemoglobin. Because this steric effect changes the mechanism of binding of carbon monoxide (but not that of oxygen), we conclude that such mechanism changes also occur in hemoprotein reactions with carbon monoxide. Whereas unstrained model compounds react with CO in water with a rate constant of  $10^7 \text{ L M}^{-1} \text{ s}^{-1}$ , strained model compounds can react with a rate constant approaching  $3 \times 10^8 \text{ L M}^{-1} \text{ s}^{-1}$  by base elimination or as low as  $\sim 10^5 \text{ L M}^{-1} \text{ s}^{-1}$  by direct association. These changes in carbon monoxide mechanisms, rates of re-



action, and affinities help to explain some of the variations in reactions of dioxygen and carbon monoxide with different hemoproteins.

We have prepared models for R-state hemoglobin sites and for fast reacting T-state sites. A detailed study of the previously reported<sup>2c,12a</sup> slow reacting T-state model will be described in a subsequent paper.

## Experimental Section

Nuclear magnetic resonance spectra were recorded on either a Varian EM-390, a Varian T-60, or a Varian HR-220 spectrometer with pulse-Fourier transformation capabilities (Nicolet Transform Corporation) using tetramethylsilane as an internal standard. Chemical shifts are reported as  $\delta$  values. Infrared spectra at ambient temperatures were obtained as Nujol mulls and recorded on a Perkin-Elmer infracord spectrophotometer or a Perkin-Elmer Model 257 grating infrared spectrophotometer. Visible spectra were recorded on a Cary Model 15 spectrophotometer. Acidity titrations were made with a Radiometer Model TTTIC pH meter.

Thin-layer chromatography plates were a product of Eastman Kodak (No. 6060, with fluorescent indicator, and No. 6061, without fluorescent indicator). Silica gel (60–200 mesh) was purchased from J. T. Baker Chemical Co. (5-3405) and was not activated prior to use.

Common solvents were used as received unless otherwise noted. Anhydrous methylene chloride and triethylamine were prepared by drying over calcium hydride. Anhydrous toluene was prepared by drying over freshly cut sodium metal. Deuteriochloroform (99.8% D, D319) was obtained from Stohler Isotope Chemicals and was stored over fresh molecular sieves.

Elementary analyses were performed by Pascher and Pascher Mikroanalytisches Laboratory, Bonn, West Germany, and Galbraith Laboratories, Knoxville, Tenn.

Compound **1**<sup>+</sup>Cl<sup>-</sup>, **2**<sup>+</sup>Cl<sup>-</sup>, **8**<sup>+</sup>Cl<sup>-</sup>, **9**<sup>+</sup>Cl<sup>-</sup>, **10**<sup>+</sup>Cl<sup>-</sup>, and mesoporphyrin monomethyl ester (**16-P**) are described elsewhere.<sup>10d</sup>

**1-(3-Aminopropyl)imidazole (17)** was prepared as previously described.<sup>10d</sup>

**Silver Imidazolate (18)**. An aqueous solution (300 mL) of imidazole (Aldrich, I20-2, 0.63 mol, 42.6 g) was mixed with an aqueous solution (360 mL) of silver nitrate (0.69 mol, 117 g), yielding a flocculant white precipitate. Aqueous ammonia (28%, 226 mL) was added and the mixture stirred for 30 min. The precipitate was collected and washed with water, ethanol, and diethyl ether and vacuum dried; yield, 96.5 g (88%).

**4-(1-Imidazolyl)butyronitrile (19)**. Silver imidazolate (**18**) (10 g, 57.5 mmol) was suspended in anhydrous toluene (100 mL) and heated to 100 °C. To the stirred solution was added 4-bromobutyronitrile (Pfaltz and Bauer, 5.97 mL, 57.5 mmol). The mixture was stirred for 24 h at 105 °C. The precipitate was filtered and washed three times with toluene (30 mL). The combined washes and the filtrate were evaporated to a yellow oil. The crude product was dissolved in benzene and loaded on a silica gel column (2 × 20 cm) packed with benzene. Elution with benzene removed any unreacted 4-bromobutyronitrile. Elution with methylene chloride removed the 4-(1-imidazolyl)butyronitrile: IR (neat) nitrile absorption at 2280 cm<sup>-1</sup>; NMR (CDCl<sub>3</sub>)  $\delta$  2.2 (t, 2 H), ~2.0 (m, 2 H), 4.0 (t, 2 H), 6.85 (s, 2 H), 7.35 (s, 1 H); yield, 0.4 g (5.2%).

**1-(4-Aminobutyl)imidazole (20)**. 4-(1-Imidazolyl)butyronitrile (**19**) (2.0 g, 14.8 mmol) was dissolved in absolute methanol (50 mL). The solution was saturated with ammonia. Freshly prepared Raney nickel<sup>6</sup> (W-7, ~1 g) was added as a methanol suspension. The reaction mixture was placed in a Parr shaker, degassed three times by evacuating and filling with hydrogen, and hydrogenated over 5 psi of pressure of hydrogen. The reaction was stopped when no further uptake of hydrogen was observed. The catalyst was filtered and the filtrate evaporated to a yellow sticky oil. The crude product was dissolved in a minimum volume of methylene chloride–tetrahydrofuran (95:5, v/v) and chromatographed on a silica gel column (1 × 10 cm). Elution with the same solvent mixture afforded the final product: IR, no absorption in nitrile region, N–H stretching at ~3400 cm<sup>-1</sup>; NMR (CDCl<sub>3</sub>)  $\delta$  1.57 (m, 4 H), 2.6 (s, 2 H), 2.62 (t, 2 H), 3.86 (t, 2 H), 6.71 (s, 2 H), 7.20 (s, 1 H); yield, 1.47 g (71%).

**1-(4-Acetylaminoethyl)imidazole (13)**. 1-(4-Aminobutyl)imidazole (**20**) (0.8 g, 784  $\mu$ L, 5.76 mmol) was suspended in anhydrous methylene chloride (10 mL). Acetic anhydride (614  $\mu$ L, 6.5 mmol) was

dissolved in anhydrous methylene chloride (5 mL) and the solution added dropwise to the amine. The mixture was stirred at room temperature for 30 min. The reaction mixture was washed twice with 1 N NaOH and three times with distilled water. Evacuation removed all volatile impurities: IR, amide carbonyl absorption at 1660 cm<sup>-1</sup>; NMR (CDCl<sub>3</sub>)  $\delta$  1.6 (m, 4 H), 1.7 (s, 3 H), 2.7 (m, 2 H), 3.75 (t, 2 H), 6.7 (s, 2 H), 7.2 (s, 1 H), 7.9 (s, 1 H); yield, 0.42 g (40%).

**2-(1-Imidazolyl)ethanol (21)**. Imidazole (Aldrich, I20-2, 20 g, 0.29 mol) and ethylene carbonate (Matheson Coleman and Bell, EX5007504, 40 g, 0.45 mol) were heated to 75 °C for 24 h, after which all carbon dioxide evolution had ceased. Fractional distillation at reduced pressure of the crude product yielded a pale yellow oil alcohol: bp 125–130 °C (~0.2 Torr); NMR (CDCl<sub>3</sub>)  $\delta$  3.8 (m, 4 H), 6.80 (s, 1 H), 6.90 (s, 1 H), 6.92 (s, 1 H), 7.35 (s, 1 H); D<sub>2</sub>O exchange of hydroxyl proton removed the hydroxyl resonance at  $\delta$  6.8; yield 17.2 g (52.3%).

**Bis[3-(1-imidazolyl)propyl]amine (22)**. 3-(1-Imidazolyl)propionitrile<sup>10d</sup> (20.3 g, 168 mmol) and freshly prepared W-2 Raney nickel (~10 g) were suspended in absolute methanol (100 mL). In order to maximize secondary amine formation, saturation of the mixture with ammonia was omitted. The reaction mixture was placed in a Parr shaker, degassed three times by evacuating and filling with hydrogen, and hydrogenated over 50 psi of pressure of hydrogen. The reaction was stopped when no further uptake of hydrogen was observed. The mixture was filtered and concentrated in vacuo. The crude product was chromatographed on an alumina column (2 × 40 cm). Elution with chloroform–methanol (95:5, v/v) yielded a mixture of unreacted starting material and secondary amine in the first fractions. The combined reactions containing secondary amine were rechromatographed on a silica gel column (2 × 40 cm). Elution with chloroform–methanol (95:5, v/v) resolved the components. The second peak eluted contained the purified secondary amine: NMR (CDCl<sub>3</sub>)  $\delta$  1.33 (s, 1 H), 1.87 (m, 4 H), 2.53 (t, 4 H), 3.99 (t, 4 H), 6.93 (d, 4 H), 7.42 (s, 2 H); yield, 2.13 g (10.8%).

**3-[1-(2-Methyl)imidazolyl]propionitrile (23)**. Acrylonitrile (50 mL) was heated to 50 °C. 2-Methylimidazole (Aldrich, 27.2 g) was added slowly with stirring. After the addition was complete the solution was refluxed for 3 h. Excess acrylonitrile was removed at reduced pressure. The oily residue was dissolved in methanol (200 mL) to which charcoal (~2 g) was added. The mixture was boiled for 10 min and filtered through Celite. Removal of methanol at reduced pressure yielded the nitrile as a colorless oil: NMR (CDCl<sub>3</sub>)  $\delta$  2.37 (s, 3 H), 2.77 (t, 2 H), 4.09 (t, 2 H), 6.83 (s, 1 H), 6.78 (s, 1 H); yield, 26.0 g (93%).

**3-[1-(2-Methyl)imidazolyl]propylamine (24)** was prepared from 3-[1-(2-methyl)imidazolyl]propionitrile (**23**) (18 g) and W-2 Raney nickel (~12 g) according to the same procedure used for **20**. After removal of catalyst and solvent the crude product was distilled at reduced pressure (130–135 °C, ~0.2 Torr): NMR (CDCl<sub>3</sub>)  $\delta$  1.82 (m, 2 H), 2.15 (s, 2 H), 2.34 (s, 3 H), 2.70 (t, 2 H), 3.92 (t, 2 H), 6.83 (s, 2 H); yield, 15.4 g (83%).

**2-(1-Imidazolyl)ethyl Acetate (12)**. 2-(1-Imidazolyl)ethanol (**21**) (7.0 g, 62.5 mmol) was dissolved in anhydrous methylene chloride (10 mL) and the reaction vessel purged with dry argon. Acetic anhydride (7.5 g, 73.5 mmol) was dissolved in anhydrous methylene chloride (25 mL) and added dropwise to the alcohol at 0 °C. The mixture was stirred for 3 h and warmed to room temperature. The acetic acid and excess acetic anhydride were removed in vacuo. Fractional distillation at reduced pressure yielded a pale yellow oil: bp 120–125 °C (~0.1 Torr); NMR (CDCl<sub>3</sub>)  $\delta$  1.97 (s, 3 H), 4.2 (m, 4 H), 6.92 (s, 1 H), 6.95 (s, 1 H), 7.4 (s, 1 H); yield, 4.2 g (44%).

**1-(3-Acetylaminoethyl)imidazole (11)**. 1-(3-Aminopropyl)imidazole (**17**) (2.0 g, 16.0 mmol) was dissolved in anhydrous methylene chloride (15 mL) and the reaction vessel purged with dry argon. Acetic anhydride (1.9 mL, 20 mmol) was dissolved in anhydrous methylene chloride (10 mL) and added dropwise to the amine at 0 °C. The mixture was stirred for 1 h and allowed to warm to room temperature. The mixture was evaporated to a sticky yellow oil in vacuo. Fractional distillation at reduced pressure afforded the final product: bp 145–150 °C (~0.1 Torr); NMR (CDCl<sub>3</sub>)  $\delta$  1.97 (s, 3 H), 2.0 (m, 2 H), 3.2 (m, 2 H), 3.95 (t, 2 H), 6.92 (s, 2 H), 7.45 (s, 1 H), 8.10 (s, 1 H); yield, 1.61 g (60.2%).

**1-(3-Acetylaminoethyl)-2-methylimidazole (14)** was synthesized from 3-[1-(2-methyl)imidazolyl]propylamine (**24**) (1 g) according to the procedure used to acetylate **13**: IR 1693 and 1563 cm<sup>-1</sup>, indicative of a secondary amide; yield, 0.5 g (40%).

**3-(3-Pyridyl)propyl Acetate (15)**. 3-(3-Pyridyl)propanol (Aldrich,

Table VII. NMR of Porphyrins in CDCl<sub>3</sub> in Units of  $\delta$  (ppm from Me<sub>4</sub>Si)

Compd	Im 2-H (2-CH <sub>3</sub> )	Im 4,5-H	$\alpha$ -CH <sub>2</sub>	$\beta$ -CH <sub>2</sub>	$\gamma$ -CH <sub>2</sub>	$\Delta$ -CH <sub>2</sub>	NH
3-P	0.23 (3, d)	4.74 <sup>a</sup> (1, s)	0.32 (2, m)	-0.31 (2, m)	2.04 (2, m)		5.69 (1, m)
4-P	0.44 (6, d)	5.32 (2, s) 5.73 (2, s)	2.14 (4, m)	0.93 (4, m)	2.82 (4, m)		7.65 (2, m)
5-P	6.90 (1, s)	7.10 (1, s) 7.17 (1, s)					
6-P	6.36 (1, s)	5.30 (1, s) 6.28 (1, s)	1.97 (2, m)		0.23 (4, m)	2.71 (2, m)	5.78 (1, m)
7-P	7.34 (1, s)	6.47 (1, s) 6.91 (1, s)	3.27 <sup>b</sup> (4, m)	1.32 (2, m)	3.09 (2, m)		
	5.96 (1, d)	4.82 (1, d) 5.78 (1, d)	2.45 (2, m)	0.75 (2, m)	2.65 (2, m)		

Compd	Meso H's	$\alpha$ -Propionic CH <sub>2</sub>	Ethyl CH <sub>2</sub>	Ring CH <sub>3</sub> + -OCH <sub>3</sub>	$\beta$ -Propionic CH <sub>2</sub>	Ethyl CH <sub>3</sub>	Pyrrole N-H
3-P	9.57-9.85 (4, m)	4.08 (4, m)	3.92 (4, m)	3.28-3.52 <sup>c</sup> (16, m)	3.18 (2, q) 2.78 (2, t)	1.77 (6, m)	-4.60 (2, s)
4-P	9.88-10.01 (4, m)	4.35 (4, m)	4.00 (4, m)	3.51-3.60 (12, m)	3.15 (4, m)	1.82 (6, d of t)	-4.68 (2, s)
5-P	10.10 (4, s)		4.05 (4, m)	3.55-3.75 (15, m)	3.25 (4, m)	1.85 (6, m)	
6-P	9.93-9.97 (4, m)	4.33 (4, m)	4.02 (4, q)	3.39-3.60 (15, m)	3.24 (2, d of t) 3.03 (2, d of t)	1.82 (6, t)	-4.08 (2, s)
7-P	9.80-9.98 (4, m)	4.30 (4, m)	3.00 (4, m)	3.42-3.58 (15, m)	3.27 (4, m) <sup>d</sup> 2.90 (2, m)	1.83 (6, t)	-4.20 (2, s)

<sup>a</sup> Other imidazole H buried under ring CH<sub>3</sub>'s. <sup>b</sup> Includes  $\beta$ -propionic CH<sub>2</sub>. <sup>c</sup> Includes imidazole H of side chain. <sup>d</sup> Includes side-chain methylene.

P7120-7, 3.0 g, 21.9 mmol) was dissolved in anhydrous methylene chloride (10 mL) and the reaction vessel purged with dry argon. Acetic anhydride (2.07 mL, 21.9 mmol) was dissolved in anhydrous methylene chloride (8 mL) and added dropwise to the alcohol at 0 °C. The mixture was stirred for 3 h and warmed to room temperature. The crude product was evaporated to a pale yellow oil. Fractional distillation at reduced pressure afforded the final product: bp 134-138 °C (~0.2 Torr); NMR (CDCl<sub>3</sub>)  $\delta$  1.94 (m, 2 H), 1.98 (s, 3 H), 2.64 (t, 2 H), 3.98 (t, 2 H), 7.2 (m, 2 H), 8.2 (m, 2 H); yield, 2.33 g (59%).

**Mesohemin Mono-2-(1-imidazolyl)ethyl Ester, Monomethyl Ester (5<sup>+</sup>Cl<sup>-</sup>).** Mesoporphyrin mono-2-(1-imidazolyl)ethyl ester, monomethyl ester (5-P), was synthesized from mesoporphyrin monomethyl ester, monoacid (16-P) (30 mg, 51.7  $\mu$ mol), pivaloyl chloride (5.3  $\mu$ L, 62  $\mu$ mol), and 2-(1-imidazolyl)ethanol (21) (7 mg, 62  $\mu$ mol), and purified according to the mixed anhydride procedure:<sup>10d</sup> visible spectrum (CHCl<sub>3</sub>) 498, 532, 566, 618 nm; IR (CH<sub>2</sub>Cl<sub>2</sub>) ester carbonyl absorption at 1730 cm<sup>-1</sup>; NMR in Table VII; yield, 25 mg (72%). Iron insertion was accomplished in the usual manner<sup>35</sup> with the purified porphyrin (25 mg). The hemin was chromatographed on a silica gel column (2  $\times$  40 cm) eluting with 9:1 (v/v) chloroform-methanol:<sup>10d,35</sup> yield, 26 mg (29%). Thin-layer chromatography showed single-spot purity with three eluting solvents having very different properties. The above eluent moves any diester rapidly and moves the ester-amide, the amide-acid, and diacid progressively slower. An 85:10:5 (v/v/v) chloroform-methanol-triethylamine eluent freezes mono- and diacids at the origin and gives an *R<sub>f</sub>* ~0.5 for the product amide-ester. Chloroform-methanol-formic acid (85:5:10, v/v/v) freezes bases such as the amide-ester product, 5<sup>+</sup>Cl<sup>-</sup>, at or near the origin and moves components having ester or acid functions.

**Mesohemin Mono-4-(1-imidazolyl)butylamide, Monomethyl Ester (6<sup>+</sup>Cl<sup>-</sup>).** Mesoporphyrin mono-4-(1-imidazolyl)butylamide, monomethyl ester (6-P), was synthesized from mesoporphyrin monomethyl ester, monoacid (36 mg, 62  $\mu$ mol), pivaloyl chloride (5.3  $\mu$ L, 62  $\mu$ mol), and 1-(4-aminobutyl)imidazole (20) (8.5  $\mu$ L, 62.3  $\mu$ mol) and purified according to the mixed anhydride procedure:<sup>10d</sup> NMR in Table VII; yield, 24 mg (55%). Iron insertion was accomplished in the usual manner<sup>35</sup> with the purified porphyrin (24 mg) and the hemin chromatographed and checked for purity as described above: yield, 20 mg (74%).

**Mesohemin Mono-3-[1-(2-methyl)imidazolyl]propylamide, Monomethyl Ester (3<sup>+</sup>Cl<sup>-</sup>).** Mesoporphyrin mono-3-[1-(2-methyl)imidazolyl]propylamide, monomethyl ester (3-P), was synthesized from mesoporphyrin monomethyl ester, monoacid (16-P) (20 mg, 34  $\mu$ mol), pivaloyl chloride (6  $\mu$ L, 50  $\mu$ mol), and 3-[1-(2-methyl)imidazolyl]-

propylamine (24) (5.8 mg, 42  $\mu$ mol) and purified according to the mixed anhydride procedure:<sup>10d</sup> NMR in Table VII. Iron insertion was accomplished in the usual manner<sup>35</sup> with the purified porphyrin. The hemin was chromatographed and checked for purity as described above: yield, 6 mg (22%).

**Mesohemin Di-3-[1-(2-methyl)imidazolyl]propylamide (4<sup>+</sup>Cl<sup>-</sup>).** Mesoporphyrin (3-[1-(2-methyl)imidazolyl]propylamide (4-P) was synthesized from mesoporphyrin (116 mg, 205  $\mu$ mol), pivaloyl chloride (71  $\mu$ L, 589  $\mu$ mol), and 3-[1-(2-methyl)imidazolyl]propylamine (24) (79 mg, 568  $\mu$ mol) and purified by the mixed anhydride procedure described above: NMR in Table VII. Iron insertion was accomplished in the usual manner<sup>35</sup> with the purified porphyrin. The hemin was chromatographed and checked for purity as described above: yield, 8 mg (15%).

**Mesohemin Mono[bis[3-(1-imidazolyl)propyl]amide), Monomethyl Ester (7<sup>+</sup>Cl<sup>-</sup>).** Mesoporphyrin mono[bis[3-(1-imidazolyl)propyl]amide), monomethyl ester (7-P), and mesoporphyrin di[bis[3-(1-imidazolyl)propyl]amide) (25-P) were synthesized from mesoporphyrin diacid (327 mg, 576  $\mu$ mol), pivaloyl chloride (140  $\mu$ L, 1162  $\mu$ mol), and bis[3-(1-imidazolyl)propyl]amide (22) (144 mg, 618  $\mu$ mol) by a modification of the mixed anhydride method. After the amine was added the reaction was quenched with methanol (20 mL) to convert unreacted mixed anhydride to methyl ester. This gave a statistical distribution of products (~25% 8-P, ~50% 7-P, ~25% 25-P). 7-P was isolated by chromatography of the reaction mixture on a silica gel column (2  $\times$  40 cm). Elution with chloroform-methanol (95:5, v/v) cleanly removed the purified porphyrin: NMR in Table VII; yield, 144 mg (31%). Iron insertion was accomplished in the usual manner. The hemin was chromatographed in the usual manner: yield, 65 mg (42%).

**pK<sub>a</sub> Measurements.** Acid dissociation constants were obtained by titration of an aqueous solution of the base (~0.05 mequiv of base, ~10 mL of glass-distilled water, pH 7.0) with hydrochloric acid (4 N). The pH of the solution was recorded after each addition of acid. Titration curves were plotted and the end point taken as the inflection point of these curves. The acid dissociation constant (pK<sub>a</sub>) was taken as the pH at half-titration. The pK<sub>a</sub> values reported in Table VII are the average of a minimum of five titrations.

**pH-Rate Profile.** Hemins from Table I were suspended in 10 mL of potassium phosphate (dibasic, 0.1 M), containing 2% CetMe<sub>3</sub>NBr and reduced with sodium dithionite.<sup>10g</sup> Aliquots of degassed (3  $\times$  freeze-thaw) phosphoric acid (10%) were injected via a gas-tight microliter syringe to effect pH changes. The volume of phosphoric acid requisite for a given 0.5 pH-unit change was determined in a

separate experiment, measuring the pH of the heme suspension as a function of the volume of phosphoric acid added. The identical pH changes could thus be effected anaerobically within the cuvette previously described.<sup>10d</sup> The second-order carbon monoxide rate constants were then obtained at each pH by the usual flash photolysis technique. At the conclusion of the pH-rate profile, the pH of the solution was measured to verify that the final pH was correct. In these experiments heme concentrations were 2–7  $\mu\text{M}$  and carbon monoxide concentrations were 15–30  $\mu\text{M}$ . The methods of determining the kinetics of reversible reaction of dioxygen with the chelated hemes have been described in detail.<sup>10c,d</sup>

**Titration of Hemes with Carbon Monoxide.** Carbon monoxide binding to hemes was followed by observing optical density changes at the heme Soret absorption. Titrations were performed with 10 mL of the heme solution (8  $\mu\text{M}$ ) in 2%  $\text{CetMe}_3\text{NBr}$ -0.1 M phosphate buffer, pH 7.3, in a tonometer similar to that previously described,<sup>10d</sup> which consisted of a cuvette attached to a bulb and a stopcock, such that the volume of the entire apparatus was 550  $\text{cm}^3$ . A calibrated space between stopcocks allows 0.45 mL of gas at a measured pressure to be admitted. The CO could then be swept and expanded into the evacuated tonometer by a pulse of argon, thus obtaining a known pressure of CO over the solution. Each addition introduced an amount of CO which was at least five times the amount of heme present. After stirring and shaking for at least 10 min, the spectrum was recorded. This operation was repeated for successive additions of CO, thus obtaining  $P_{1/2} = 0.25$  Torr for **3**. This method affords only a lower limit for  $K_{\text{CO}}$  values which are greater than  $10^7 \text{ M}^{-1}$ .

**Acknowledgment.** We are grateful to Dr. V. S. Sharma and Professor Q. H. Gibson for helpful discussions.

## References and Notes

- (1) The National Institutes of Health supported this research (Grant No. HL-13581) and the NMR facilities which were used (Grant No. RR-00708).
- (2) (a) Some of these results were previously communicated in preliminary form; (b) J. Geibel, C. K. Chang, and T. G. Traylor, *J. Am. Chem. Soc.*, **97**, 5924 (1975); (c) J. Cannon, J. Geibel, M. Whipple, and T. G. Traylor, *ibid.*, **98**, 3395 (1976).
- (3) See also J. Geibel, Ph.D. Thesis, University of California, San Diego, Calif., 1976.
- (4) F. Antonini and M. Brunori, "Hemoglobin and Myoglobin and Their Reactions with Ligands", North Holland Publishing Co., Amsterdam, 1971, p. 1.
- (5) See ref 4, p 220.
- (6) D. E. Koshland, G. Menethy, and D. Filmer, *Biochemistry*, **5**, 365 (1966).
- (7) (a) M. F. Perutz, J. E. Ladner, S. R. Simon, and C. Ho, *Biochemistry*, **13**, 2174 (1974); (b) M. F. Perutz, J. E. Ladner, J. G. Bettlesome, C. Ho, and E. F. Slade, *ibid.*, **13**, 2187 (1974).

- (8) J. Monod, J. Wyman, and J. P. Changeux, *J. Mol. Biol.*, **12**, 88 (1965).
- (9) J. J. Hopfield, *J. Mol. Biol.*, **77**, 207 (1973).
- (10) (a) C. K. Chang and T. G. Traylor, *J. Am. Chem. Soc.*, **95**, 5810 (1973); (b) C. K. Chang and T. G. Traylor, *Proc. Natl. Acad. Sci. U.S.A.*, **70**, 2647 (1973); (c) C. K. Chang and T. G. Traylor, *ibid.*, **72**, 1166 (1975); (d) T. G. Traylor, C. K. Chang, J. Geibel, T. Mincey, J. Cannon, and A. Berzini, *J. Am. Chem. Soc.*, submitted for publication; (e) W. S. Brinigar, C. K. Chang, J. Geibel, and T. G. Traylor, *ibid.*, **96**, 5597 (1974); (f) J. F. Geibel, T. G. Traylor, V. S. Sharma, and H. M. Ranney, unpublished results; (g) C. K. Chang and T. G. Traylor, *J. Am. Chem. Soc.*, **98**, 6765 (1976); (h) D. Campbell, unpublished results.
- (11) R. W. Noble and W. H. Gibson, *J. Biol. Chem.*, **244**, 3905 (1969).
- (12) (a) The reduced CO binding constant for deuteroheme-2-methylimidazole mixtures as compared with imidazole-deuteroheme mixtures observed by Brault and Rougee provides one example of the effect of such steric effects on ligation; (b) M. Rougee and D. Brault, *Biochemistry*, **14**, 4100 (1975); (c) D. Brault and M. Rougee, *Biochem. Biophys. Res. Commun.*, **57**, 654 (1974); (d) D. Brault and M. Rougee, *Biochemistry*, **13**, 4598 (1974), and references therein.
- (13) G. P. Wagner and R. J. Kassner, *Biochim. Biophys. Acta*, **392**, 319 (1975).
- (14) J. Cannon, J. Geibel, and D. White, unpublished data.
- (15) M. Eigen, *Angew. Chem.*, **3**, 1 (1963).
- (16) J. H. Fendler and E. J. Fendler, "Catalysis in Micellar and Macromolecular Systems", Academic Press, New York, N.Y., 1975, Chapter 6.
- (17) A. Warshel, *Proc. Natl. Acad. Sci. U.S.A.*, **74**, 1789 (1977).
- (18) J. L. Hoard, *Science*, **174**, 1295 (1971).
- (19) E. J. Heidner, R. C. Ladner, and M. F. Perutz, *J. Mol. Biol.*, **104**, 707 (1976).
- (20) R. Huber, O. Epp, and H. Formanek, *J. Mol. Biol.*, **52**, 349 (1970).
- (21) (a) M. Perutz, J. V. Kilmartin, K. Nagai, A. Szabo, and S. R. Simon, *Biochemistry*, **15**, 378 (1976); (b) A. Szabo and M. F. Perutz, *ibid.*, **14**, 4427 (1976).
- (22) J. C. Maxwell and W. S. Caughey, *Biochemistry*, **15**, 388 (1976).
- (23) G. Giacometti, E. Antonini, and T. G. Traylor, *J. Biol. Chem.*, in press.
- (24) J. C. Nowell, A. C. Nunes, and B. P. Schoenborn, *Science*, **190**, 568 (1975).
- (25) (a) W. S. Caughey, *Ann. N.Y. Acad. Sci.*, **174**, 148 (1970); (b) S. Yoshikawa, M. G. Choc, M. C. O'Toole, and W. S. Caughey, *J. Biol. Chem.*, **252**, 5498 (1977).
- (26) G. Amiconi, E. Antonini, M. Brunori, H. Formanek, and R. Huber, *Eur. J. Biochem.*, **31**, 52 (1972).
- (27) J. Blanck, K. Ruckpaul, W. Schleyer, and F. Jung, *Eur. J. Biochem.*, **25**, 476 (1972).
- (28) M. Brunori and T. M. Schuster, *J. Biol. Chem.*, **244**, 4046 (1969).
- (29) E. Antonini, *Physiol. Rev.*, **45**, 123 (1965).
- (30) T. Imamura, A. Riggs, and W. H. Gibson, *J. Biol. Chem.*, **247**, 521 (1972).
- (31) J. Wittenberg, C. A. Appleby, and B. A. Wittenberg, *J. Biol. Chem.*, **247**, 527 (1972).
- (32) W. H. Gibson, *Proc. Natl. Acad. Sci. U.S.A.*, **70**, 1 (1973).
- (33) V. S. Sharma, M. R. Schmidt, and H. M. Ranney, *J. Biol. Chem.*, **251**, 4267 (1976).
- (34) (a) R. MacQuarrie and Q. H. Gibson, *J. Biol. Chem.*, **246**, 5832 (1971); (b) Q. H. Gibson, *ibid.*, **245**, 3285 (1971).
- (35) J. E. Falk, "The Porphyrins and Metalloporphyrins", Elsevier, New York, N.Y., 1964, p. 52.

## Avidin-Biotin Affinity Columns. General Methods for Attaching Biotin to Peptides and Proteins

Klaus Hofmann,\* Frances M. Finn, and Yoshiaki Kiso

Contribution from the Protein Research Laboratory, University of Pittsburgh School of Medicine, Pittsburgh, Pennsylvania 15261 (K.H.), and The Deutsches Wollforschungsinstitut an der Rheinisch-Westfälischen Technischen Hochschule, D-51 Aachen, Federal Republic of Germany. Received October 26, 1977

**Abstract:** The A-B catch principle is a novel technique for the preparation of affinity columns that is based on the high affinity of the B-complex vitamin biotin for the egg-white protein avidin. One advantage of the technique involves the attachment of biotin to biologically active molecules in a targeted manner that does not impair biological activity. This communication relates synthetic routes by biocytinamide and to  $N^\alpha$ -*p*-aminobenzoylbiocytinamide, two compounds that are useful for the biotinylation of biologically active molecules. Also described is a synthetic route to [25-biocytin]-ACTH<sub>1-25</sub>-amide, a biotinylated derivative of ACTH<sub>1-24</sub>. This compound exhibits the same adrenocortical potency with isolated bovine adrenocortical cells as the parent compound, and binds to avidin attached to Sepharose 4B.

In two previous communications<sup>1,2</sup> we have presented a novel approach to affinity columns for receptor studies which appears to be broadly applicable. This technique is based on

the remarkably strong noncovalent interaction between the B-complex vitamin biotin and the egg-white protein avidin ( $K_D \approx 10^{-15} \text{ M}$ ). The basic steps of the procedure are outlined in